

RECORDS ADMINISTRATION



R0139003

DP -467 ✓

Physics and Mathematics

AEC Research and Development Report

**NEUTRON FLUX DISTRIBUTIONS
IN NATURAL URANIUM TUBES**

by

T. B. Ponder

Experimental Physics Division

March 1960

RECORD
COPY

DO NOT RELEASE
FROM FILE

E. I. du Pont de Nemours & Co.
Savannah River Laboratory
Aiken, South Carolina

This report was prepared as an account of Government sponsored work. Neither the United States, nor the Commission, nor any person acting on behalf of the Commission:

- A. Makes any warranty or representation, expressed or implied, with respect to the accuracy, completeness, or usefulness of the information contained in this report, or that the use of any information, apparatus, method, or process disclosed in this report may not infringe privately owned rights; or
- B. Assumes any liabilities with respect to the use of, or for damages resulting from the use of any information, apparatus, method, or process disclosed in this report.

As used in the above, "person acting on behalf of the Commission" includes any employee or contractor of the Commission, or employee of such contractor, to the extent that such employee or contractor of the Commission, or employee of such contractor prepares, disseminates, or provides access to, any information pursuant to his employment or contract with the Commission, or his employment with such contractor.

Printed in USA. Price \$1.00
Available from the Office of Technical Services
U. S. Department of Commerce
Washington 25, D. C.

DP - 467

PHYSICS AND MATHEMATICS
(TID-4500, 15th Ed.)

**NEUTRON FLUX DISTRIBUTIONS
IN NATURAL URANIUM TUBES**

by

Thomas B. Ponder

March 1960

This work was done in partial fulfillment
of requirements for the degree of Master
of Science at Clemson College.

E. I. du Pont de Nemours & Co.
Explosives Department - Atomic Energy Division
Technical Division - Savannah River Laboratory

Printed for
The United States Atomic Energy Commission
Contract AT(07-2)-1

Approved by
J. L. Crandall, Research Manager
Experimental Physics Division

ABSTRACT

Measurements were made in the Process Development Pile (PDP) of the distribution of the thermal neutron flux in ten different D₂O-moderated lattices of natural uranium tubes. Both single and double fuel tubes were used at lattice spacings of 7 and 14 inches. Special corrections were required for epithermal flux shielding by the manganese detector foils. After these corrections were applied, good agreement was obtained between the measured flux distributions and corresponding distributions calculated by the P₃ approximation to transport theory.

CONTENTS

	<u>Page</u>
List of Figures	4
Introduction	5
Summary	5
Discussion	6
Description of Fuel Assemblies	6
Detailed Flux Measurements	6
Flux Calculations	7
Results	8
Flux Distributions	8
Calculation of the Average Flux	8
Calculation of Lattice Constants	8
Bibliography	10
Appendix	11

LIST OF TABLES

Table

I	Dimensions of Experimental Fuel Assemblies	12
II	Properties of Fuel Assembly Materials	12
III	Average Relative Flux Values in Experimental Assemblies	13
IV	Individual Diffusion Coefficients used to Calculate the Average Diffusion Coefficient for the Cell	13
V	Comparison of Experimental and Theoretical Values of Lattice Parameters	14

LIST OF FIGURES

<u>Figure</u>		<u>Page</u>
1	Partial Length Components of a Single Fuel Tube Assembly Showing the Windows Cut for Detailed Flux Measurements	15
2	Partial Length Components of a Double Fuel Tube Assembly Showing the Windows Cut for Detailed Flux Measurements	15
3	Cross-Sectional View of a Tubular Fuel Assembly Showing Position of Foils and Foil Holders	16
4	Experimental Apparatus for Detailed Flux Measurements in a Double Fuel Tube Assembly	17
5	Experimental and Theoretical Flux Distributions - Case 1	18
6	Experimental and Theoretical Flux Distributions - Case 2	19
7	Experimental and Theoretical Flux Distributions - Case 3	20
8	Experimental and Theoretical Flux Distributions - Case 4	21
9	Experimental and Theoretical Flux Distributions - Case 5	22
10	Experimental and Theoretical Flux Distributions - Case 6	23
11	Experimental and Theoretical Flux Distributions - Case 7	24
12	Experimental and Theoretical Flux Distributions - Case 8	25
13	Experimental and Theoretical Flux Distributions - Case 9	26
14	Experimental and Theoretical Flux Distributions - Case 10	27
15	Apparent Epithermal Flux Distribution in the Fuel Region Traversed with Manganese Detectors	28

NEUTRON FLUX DISTRIBUTIONS IN NATURAL URANIUM TUBES

INTRODUCTION

Past experience with the calculation of thermal neutron flux distributions by the P_3 approximation to transport theory has shown generally good agreement between the calculated flux distributions and those measured experimentally in reactor lattice cells^(1,2). However, most such comparisons made to date have been incidental to the course of other experiments rather than detailed tests of the theory. The purpose of the experiments described in this report was to provide just such detailed tests in D_2O -moderated lattices of natural uranium tubes. Because of radial symmetry, these lattices are particularly convenient for calculations. They are also of practical interest as possible power reactor designs⁽³⁾.

The experimental measurements of the flux distributions were made in partial loadings of the Process Development Pile (PDP), a D_2O -moderated reactor approximately 16 feet in diameter and 15 feet high⁽⁴⁾. The accompanying P_3 calculations were made on an IBM 650 computer with an existing code⁽⁵⁾ originally developed by John W. Weil at KAPL⁽²⁾.

SUMMARY

Flux distributions were measured for ten different lattices. Four of the lattices contained single fuel tubes of natural uranium metal approximately 3.5 inches in diameter with wall thicknesses ranging from 0.20 to 0.27 inch. The other six lattices contained double fuel tubes; the inner fuel tubes were approximately 2.5 inches in diameter with wall thicknesses ranging from 0.18 to 0.22 inch, while the outer fuel tubes were approximately 3.5 inches in diameter with wall thicknesses that varied from 0.18 to 0.25 inch. All experiments were made at a moderator purity of 99.34% D_2O .

The experimental flux distributions agreed well with flux distributions calculated by the P_3 method. Consequently, there was also good agreement between values of the lattice constants determined from the experimental flux distributions and those determined from the P_3 calculations. The differences in the thermal utilization, f , were within $\pm 0.3\%$ for all cases, while the values of the thermal diffusion areas, L^2 , agreed to within $\pm 4\%$.

In the cell calculations the source term for thermal neutrons, i.e., the slowing down distribution, was assumed to be uniform over the lattice cell. An attempt was made to determine the validity of this assumption for wide lattice spacings. Deliberate changes of the source term for the P_3 input and also subsequent measurements of the actual slowing down distributions with resonant detectors showed that the possible error that would result from the use of a constant source would be very small.

DISCUSSION

DESCRIPTION OF FUEL ASSEMBLIES

The fuel assemblies consisted of unclad tubes of natural uranium metal with aluminum inner and outer housings. The dimensions of the assemblies are listed in Table I. Seven different sizes of fuel tubes were used in the ten lattice cases that were studied. Four of the ten cases utilized single tubes, while in the remainder two concentric fuel tubes were utilized. Both inner and outer housing tubes were fabricated from 6063 aluminum alloy, except in lattice cases 2 and 5, where the inner housing tubes were fabricated from 6061 aluminum alloy. Properties of the fuel assembly materials are given in Table II.

Seven fuel assemblies were available for the partial loading of each lattice in the PDP. One of the seven assemblies in each case was modified for experimental procedures by cutting "windows" in the aluminum housings and the uranium tubes. Figure 1 shows pieces cut from a single fuel tube assembly with the experimental "windows". Figure 2 shows the same thing for a double fuel tube assembly.

DETAILED FLUX MEASUREMENTS

To measure the detailed flux distributions through the fuel tubes and in the moderator, manganese foils*, 0.25 inch in diameter and 0.006 inch thick, were placed in these regions and their gamma activities were counted after irradiation.

The apparatus with which flux traverses were made in one of the double fuel tube lattices is shown in Figures 3 and 4. In the moderator the manganese foils were held on aluminum "ladders" that extended out through the cell boundaries as well as into the water space at the center of the fuel tubes. In the fuel the foils were held in specially machined natural uranium "window" inserts that fit the "window" gaps in the modified fuel tubes. Holes drilled through the "window" inserts were tightly filled with stacks of the manganese foils and natural uranium spacers. Aluminum catcher foils, 0.001 inch thick were also used. They were placed between the measuring foils and the uranium to prevent pickup of radioactive fission fragments by the manganese.

*The manganese was in the form of a commercial alloy named "P-Metal". This alloy contains 72% manganese, 18% copper, and 10% nickel.

To obtain an experimental flux traverse through a lattice cell the seven tubular assemblies required for that lattice were loaded into the central test region of the PDP and the test assembly that contained the foils was placed in the center position. The remainder of the PDP tank was occupied by a reference lattice that incorporated a buffer zone to reduce flux transients at the boundary of the test lattice. The reactor was brought critical, and the foils were irradiated for 30 minutes. The foils were then unloaded and the gamma rays from the decay of the activated manganese were counted with a scintillation counter. The discriminator bias of the counter was set so that only gamma radiation above 700 kev was recorded.* The raw data was corrected for foil decay, counter background, and foil weight. To obtain the true thermal flux distribution, a correction was required for foil activations produced by epithermal neutrons. The epithermal flux correction was determined by measuring the activation of foils that had been covered with 0.030-inch-thick cadmium to stop thermal neutrons. In the moderator, the epithermal flux activation was very nearly uniform and equal to approximately 8.5% of the activity of a bare foil at the edge of the cell. The exact corrections varied slightly from case to case and were applied individually. The procedure used for determining the epithermal correction within the fuel assemblies was more involved and is given in the Appendix.

Still another correction was required to account for the superposition of the over-all reactor flux distribution on the individual lattice cell distributions. This correction proved to be insignificant, i.e., less than 0.1%, in the 7-inch lattice cases. However, it amounted to as much as 2% at the cell boundary for the 14-inch lattices.

FLUX CALCULATIONS

The flux distributions were calculated by the P_0 approximation to transport theory⁽⁵⁾. The formulation used was originally developed by J. W. Weil⁽²⁾. He obtained his basic equations by expanding the one-velocity Boltzmann equation in spherical harmonic tensor notation. Next he specialized to cylindrical coordinates, retaining terms to the third order in the Legendre polynomials of the harmonic expansion, and obtained equations for the nonvanishing tensor components. These equations were then put into a matrix form that was particularly suitable for machine computation, and the problem was coded for solution on an IBM 650 computer. The present IBM code will accommodate up to 25 annular regions and will solve a typical problem in about 2 minutes of machine time per region.

*Under these conditions only the manganese activations were counted, as determined from half-life and gamma ray spectrum measurements.

In the present code, a uniform slowing down distribution is assumed over the lattice cell. It is unlikely that this assumption is strictly true for wide lattice spacings. To determine the magnitude of the errors that it engenders changes were made in the source term for the P_s input. At the wide lattice spacings a 50% decrease of the source term in the outer half of the moderator region showed a decrease of only 5% in the thermal flux at the cell boundary. Since subsequent measurements of the actual slowing down distribution using resonance detectors showed a maximum decrease of 15% in the source term, these results indicate that the error made in assuming a constant source in flux calculations is small, at least for lattice pitches up 14 inches.

RESULTS

FLUX DISTRIBUTIONS

The experimental thermal neutron flux distributions for the various lattices are plotted against the cell radii in Figures 5 through 14. The results of the corresponding P_s calculations are also given on the figures. In each case flux values were normalized by setting the average flux in the fuel equal to one. Figures 4 and 10 cover lattices with triangular lattice pitch of 14 inches center-to-center; the remainder represent measurements made with a 7-inch lattice pitch.

CALCULATION OF THE AVERAGE FLUX

The average flux in the k^{th} component (fuel, moderator, or aluminum) of each lattice was calculated from the relation,

$$\bar{\phi}_k = \frac{\sum_1 \phi_1 \left[(r_1 + \Delta r)^2 - r_1^2 \right]}{\sum_1 \left[(r_1 + \Delta r)^2 - r_1^2 \right]}$$

where r_1 is a radius, Δr an incremental radius, and ϕ_1 is the average flux between r_1 and $r_1 + \Delta r$. These average flux values are given in Table III. All values are normalized to give an average flux of unity in the fuel.

CALCULATION OF LATTICE CONSTANTS

The average flux in each region relative to the average flux over the whole cell; i.e., the disadvantage factor of each region, was evaluated from the average flux data. It was then possible to obtain the effective absorption cross sections, Σ_a^{eff} , for the different lattice cells by the relation,

$$\Sigma_a^{\text{eff}} = \sum_i d_i \Sigma_a^i (V_i/V_{\text{cell}})$$

where d_i is the disadvantage factor of the i^{th} region, Σ_a^i is its macroscopic absorption cross section, and V_i/V_{cell} is the volume fraction of the cell occupied by the i^{th} component.

Values of the thermal utilization, f , were obtained from the results of the Σ_a^{eff} calculations. The thermal utilization is the number of thermal neutrons absorbed in the fuel relative to the total number absorbed in the cell. It is given in terms of Σ_a^{eff} as

$$f = \frac{(\Sigma_a V/V_{\text{cell}})_{\text{fuel}}}{\Sigma_a^{\text{eff}}}$$

The thermal diffusion area, L^2 , was determined by dividing the effective absorption cross section of the cell, Σ_a^{eff} , into the diffusion coefficient, D . The relation used for obtaining D for the cell, together with numerical constants used, is given in Table IV.

Table V gives a summary of the lattice constants obtained from both the experimental and the theoretical flux distributions. Generally good agreement between the two methods is evident.

T. B. Ponder (1974)

T. B. Ponder
Experimental Physics Division

BIBLIOGRAPHY

1. Dessauer, G., "Physics of Natural Uranium Lattices in Heavy Water." Proc. U. N. Intern. Conf. Peaceful Uses Atomic Energy, 2nd, Geneva, 1958, 12, 320-40 (1958). P/590
2. Weil, J. W., Neutron Flux Distribution Calculations Using the P_a Spherical Harmonic Method. General Electric Company, Schenectady, N. Y. AEC Research and Development Report KAPL-1173, 32 pp. (1954)(Confidential).
3. Babcock, D. F., Coordinator, Heavy Water Moderated Power Reactors, Quarterly Progress Report. E. I. du Pont de Nemours and Company, Wilmington, Del. AEC Research and Development Report DP-345, 60 pp. (1959).
4. Nuclear Reactor Plant Data Vol II. "Research and Test Reactors." New York: McGraw-Hill, pp 120-122 (1959).
5. Haefner, R. R., A Multigroup P_a Program for the Neutron Transport Equation. E. I. du Pont de Nemours and Company, Aiken, S. C. AEC Research and Development Report DP-427, 62 pp. (1959).

APPENDIX

Manganese has a number of sharp peaks in its curve of cross section versus neutron energy; consequently, the manganese foils used as flux detectors exhibit a comparatively strong self-shielding effect with neutrons at resonance energies. In instances where the manganese foils were closely grouped, as in the fuel regions, the number of epithermal activations depended not only on the epithermal flux distribution, but also on this self-shielding effect.

A supplementary experiment was performed to evaluate the effect within the fuel regions. A uranium "window insert" of the type used in the flux measurements was loaded with a stack of manganese foils and covered with 0.030 inch of cadmium. After an irradiation in the PDP, the gamma activity of the foils was counted. Background, decay, and weight corrections were made, and the results were plotted as epithermal neutron flux versus the distance across the "window insert".

Figure 15 shows that the epithermal flux as determined by this method appears not to be uniform, but is depressed appreciably at the center of the stack of foils. The maximum depression is reached after two foil thicknesses. These data were used to determine the corrections to be made for epithermal activations in the fuel regions. Control experiments made with uranium detector foils and with a reduced number of manganese foils did not show the epithermal flux depression, demonstrating that the effect was actually due to self-shielding in the manganese rather than being connected with epithermal absorption in the uranium.

TABLE I
DIMENSIONS OF EXPERIMENTAL FUEL ASSEMBLIES
(Dimensions, inches)

Assemblies with Single Fuel Tubes

Case No.	Component					
	Inner Process Tube		Fuel		Outer Process Tube	
	ID	OD	ID	OD	ID	OD
1	2.150	2.250	3.050	3.590	3.900	4.010
2	1.500	1.625	2.940	3.440	3.900	4.010
3	2.914	3.000	3.050	3.460	3.900	4.010
4(a)	2.914	3.000	3.050	3.460	3.900	4.010

Assemblies with Double Fuel Tubes

Case No.	Component							
	Inner Process Tube		Inner Fuel		Outer Fuel		Outer Process Tube	
	ID	OD	ID	OD	ID	OD	ID	OD
5	1.500	1.625	1.760	2.119	2.940	3.440	3.900	4.010
6	0.900	1.000	1.760	2.119	2.660	3.030	3.350	3.450
7	1.830	2.000	2.200	2.600	3.050	3.460	3.900	4.010
8	0.900	1.000	1.880	2.310	2.660	3.030	3.350	3.450
9	0.900	1.000	2.200	2.600	2.660	3.030	3.350	3.450
10(a)	0.900	1.000	2.200	2.600	2.660	3.030	3.350	3.450

(a) Cases 4 and 10 utilize a 14-inch center-to-center triangular lattice pitch. All of the other cases utilize a 7-inch center-to-center triangular lattice pitch.

TABLE II
PROPERTIES OF FUEL ASSEMBLY MATERIALS

Material	ρ , grams/cm ³	$\Sigma_a^{(a)}$, cm ⁻¹
Natural uranium	18.9	0.322
D ₂ O, 99.34 mol %	1.1038	1.601 x 10 ⁻⁴
Aluminum (1100)	2.713	0.0125
Aluminum (6061)	2.713	0.0132
Aluminum (6063)	2.713	0.127

(a) Σ_a is the macroscopic absorption cross section evaluated at 2200 m/sec.

TABLE III

AVERAGE RELATIVE FLUX VALUES IN EXPERIMENTAL ASSEMBLIES
(Normalized to the Average Flux in the Fuel)

Component	Case No. (a)									
	1	2	3	4	5	6	7	8	9	10
Inner D ₂ O space	1.197	1.192	1.133	1.079	1.006	1.025	1.060	1.006	1.130	1.059
Inner process tube	1.132	1.176	1.014	0.986	0.951	1.003	1.000	0.999	1.117	1.054
D ₂ O space between inner process tube and inner fuel	1.046	1.115	0.997	0.974	0.920	0.950	0.931	0.942	1.042	0.996
Inner fuel	1.000	1.000	1.000	1.000	0.910	0.907	0.928	0.891	0.924	0.909
D ₂ O space between inner fuel and outer fuel					0.993	0.976	0.982	1.000	0.963	0.958
Outer fuel					1.039	1.061	1.072	1.109	1.076	1.091
D ₂ O space between outer fuel and outer process tube	1.140	1.203	1.187	1.164	1.280	1.270	1.313	1.310	1.264	1.315
Outer process tube	1.213	1.314	1.257	1.280	1.382	1.373	1.444	1.433	1.366	1.534
Outer D ₂ O space	1.546	1.594	1.502	1.887	1.802	1.743	1.810	1.846	1.870	2.632
Cell	1.415	1.458	1.390	1.828	1.586	1.592	1.598	1.675	1.699	2.615

(a) Refer to Table I

TABLE IV

INDIVIDUAL DIFFUSION COEFFICIENTS USED TO CALCULATE THE AVERAGE DIFFUSION COEFFICIENT FOR THE CELL

$$D_{\text{cell}} = \frac{1}{\sum_1 \frac{V_1 d_1}{D_1}}$$

where V_1 = volume fraction for the i^{th} material

d_1 = disadvantage factor

D_1 = diffusion coefficient

Material	D_1 , cm
Natural uranium	0.713
D ₂ O, 99.34 mol %	0.816
Aluminum (1100)	3.807
Aluminum (6061)	3.691
Aluminum (6063)	3.749

TABLE V
COMPARISON OF EXPERIMENTAL AND THEORETICAL VALUES OF LATTICE PARAMETERS

Case No. (a)	Lattice Constant							
	f		D, cm		$\Sigma a^{\text{eff}}, \text{cm}^{-1}$		L^2, cm^2	
	Experiment	P_s Theory	Experiment	P_s Theory	Experiment	P_s Theory	Experiment	P_s Theory
1	0.973	0.973	0.824	0.834	0.0154	0.0156	53.1	53.4
2	0.969	0.970	0.824	0.833	0.0134	0.0140	61.2	59.3
3	0.963	0.965	0.836	0.834	0.0118	0.0124	69.6	66.9
4	0.911	0.913	0.818	0.822	0.0023	0.0024	343.2	339.9
5	0.978	0.977	0.821	0.832	0.0176	0.0176	46.6	47.1
6	0.976	0.976	0.820	0.828	0.0134	0.0135	61.1	61.3
7	0.976	0.975	0.824	0.834	0.0177	0.0176	46.4	47.3
8	0.977	0.978	0.819	0.828	0.0143	0.0142	57.1	58.0
9	0.978	0.978	0.819	0.828	0.0144	0.0145	56.6	57.0
10	0.926	0.928	0.817	0.821	0.0025	0.0026	320.2	312.2

(a) Refer to Table I

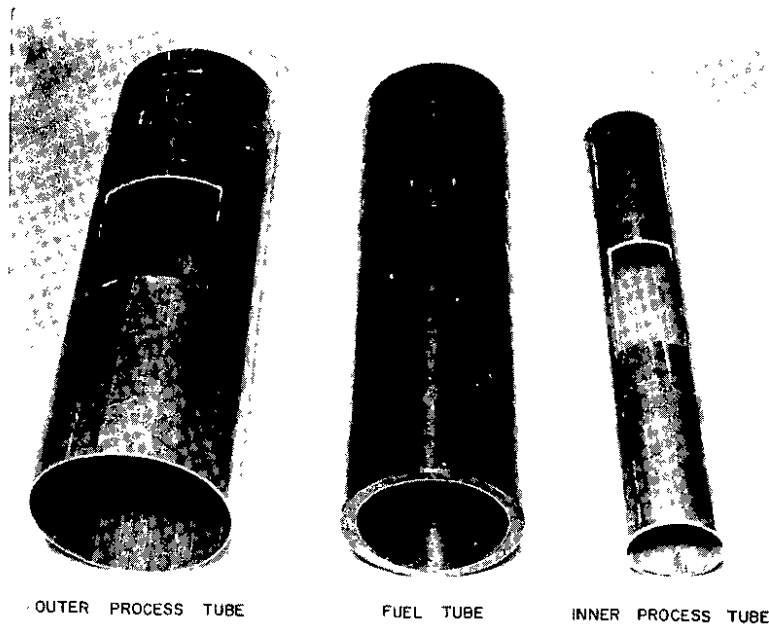


FIG. 1 PARTIAL LENGTH COMPONENTS OF A SINGLE FUEL TUBE ASSEMBLY SHOWING THE WINDOWS CUT FOR DETAILED FLUX MEASUREMENTS

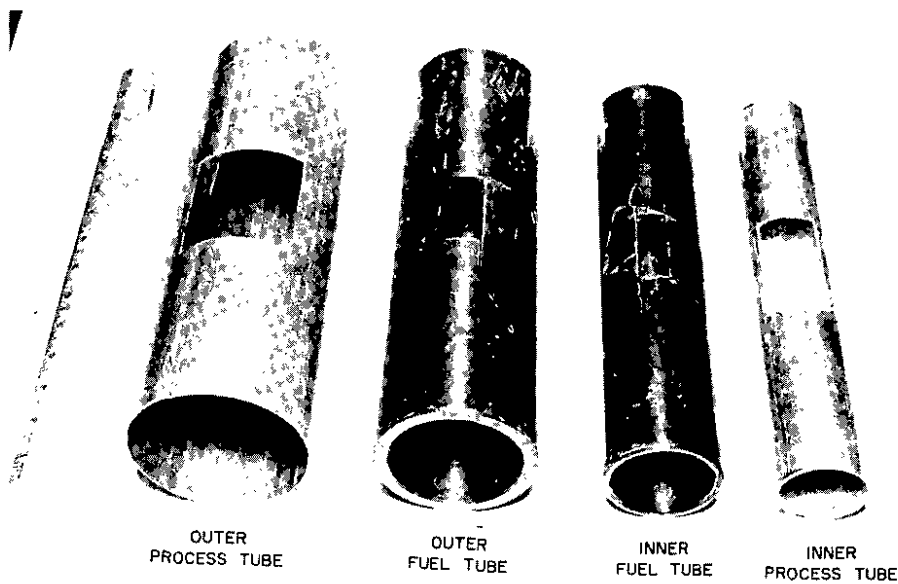


FIG. 2 PARTIAL LENGTH COMPONENTS OF A DOUBLE FUEL TUBE ASSEMBLY SHOWING THE WINDOWS CUT FOR DETAILED FLUX MEASUREMENTS

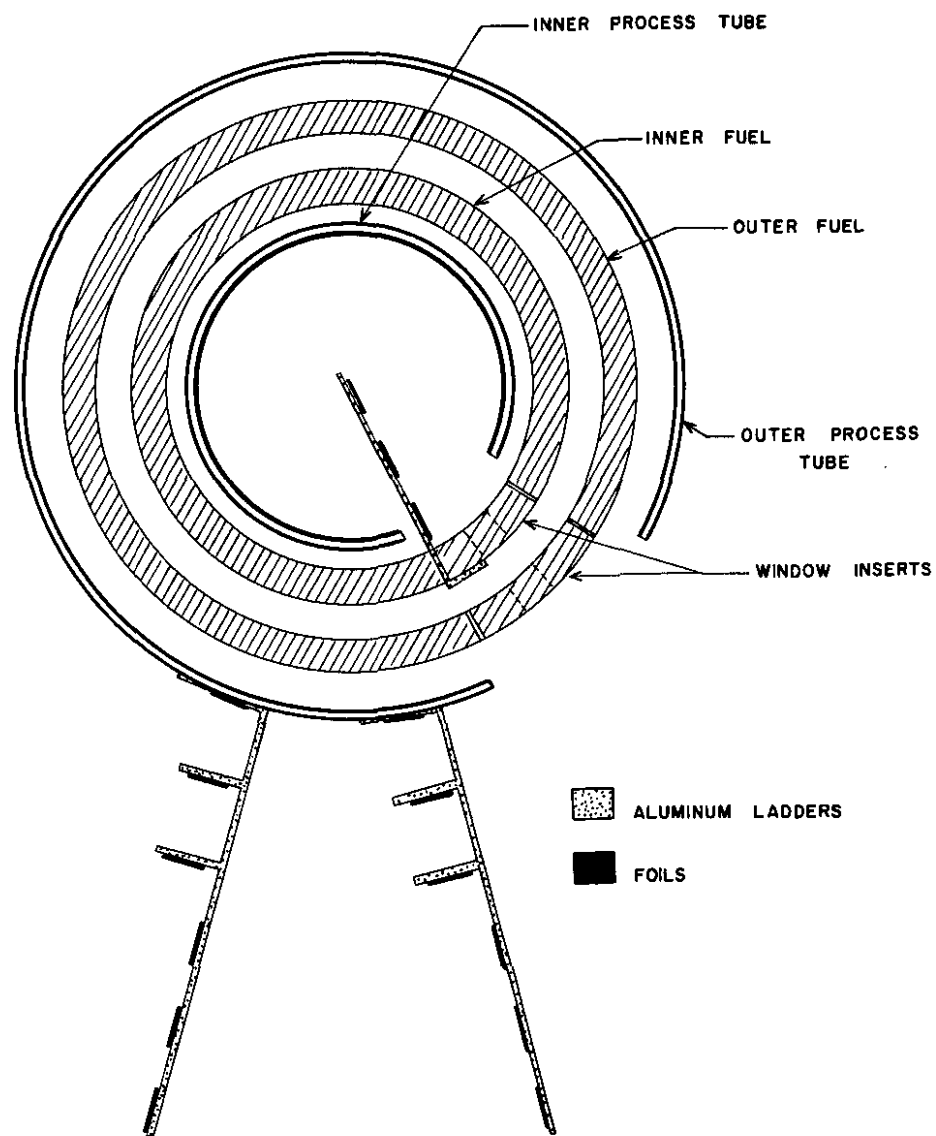


FIG. 3 CROSS-SECTIONAL VIEW OF A TUBULAR FUEL ASSEMBLY SHOWING POSITION OF FOILS AND FOIL HOLDERS

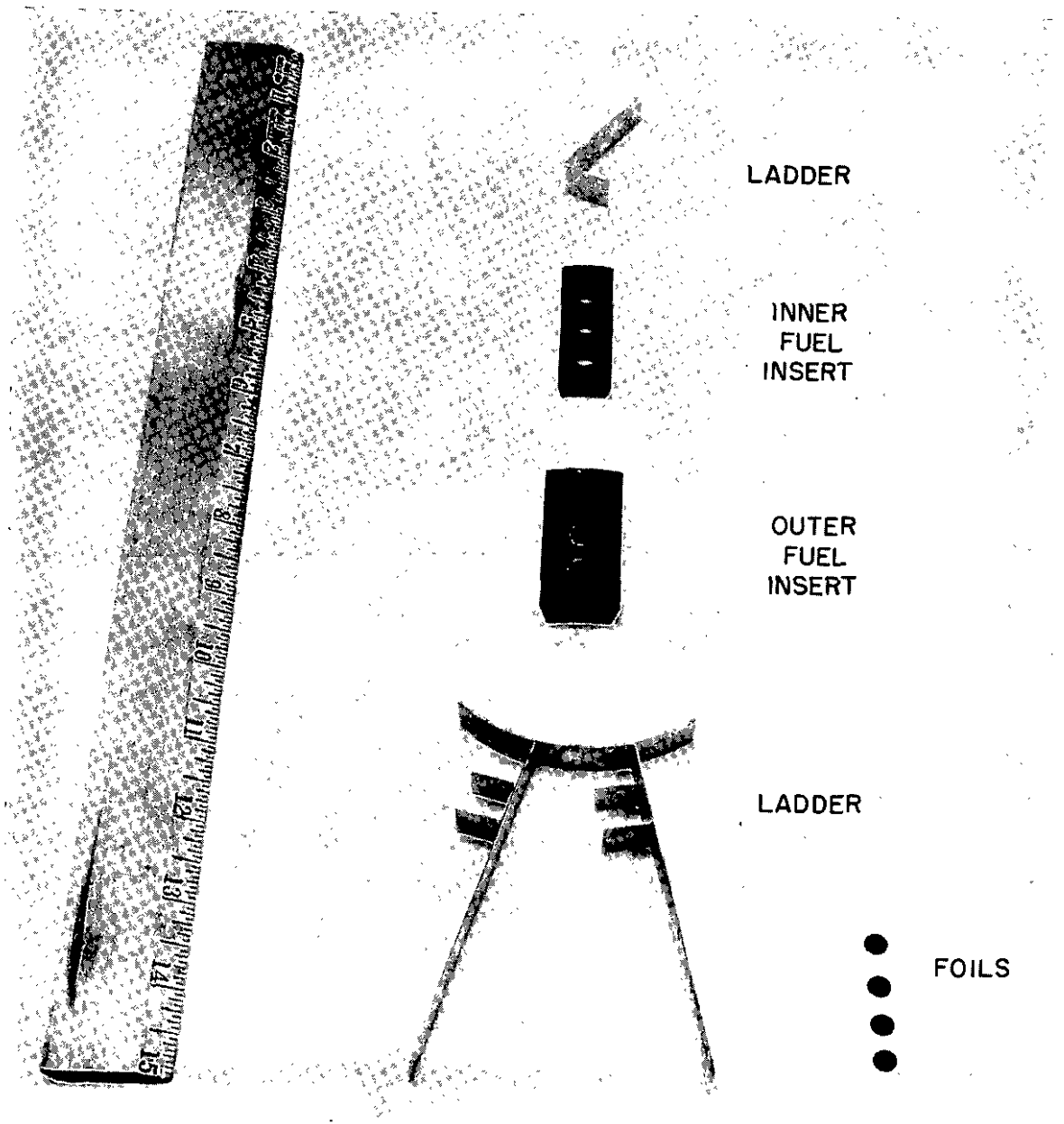


FIG. 4 EXPERIMENTAL APPARATUS FOR DETAILED FLUX MEASUREMENTS IN A DOUBLE FUEL TUBE ASSEMBLY

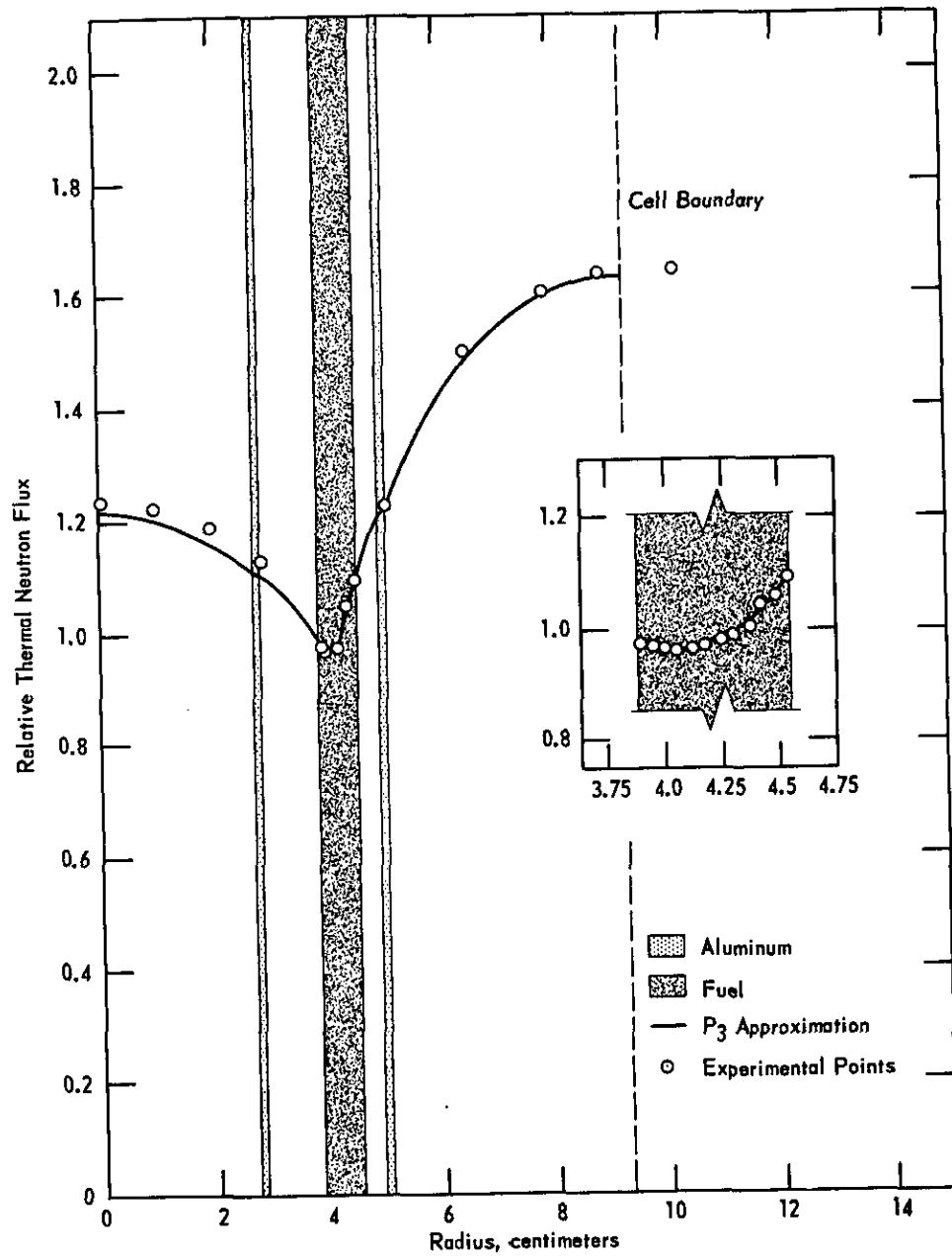


FIG. 5 EXPERIMENTAL AND THEORETICAL FLUX DISTRIBUTIONS - CASE 1

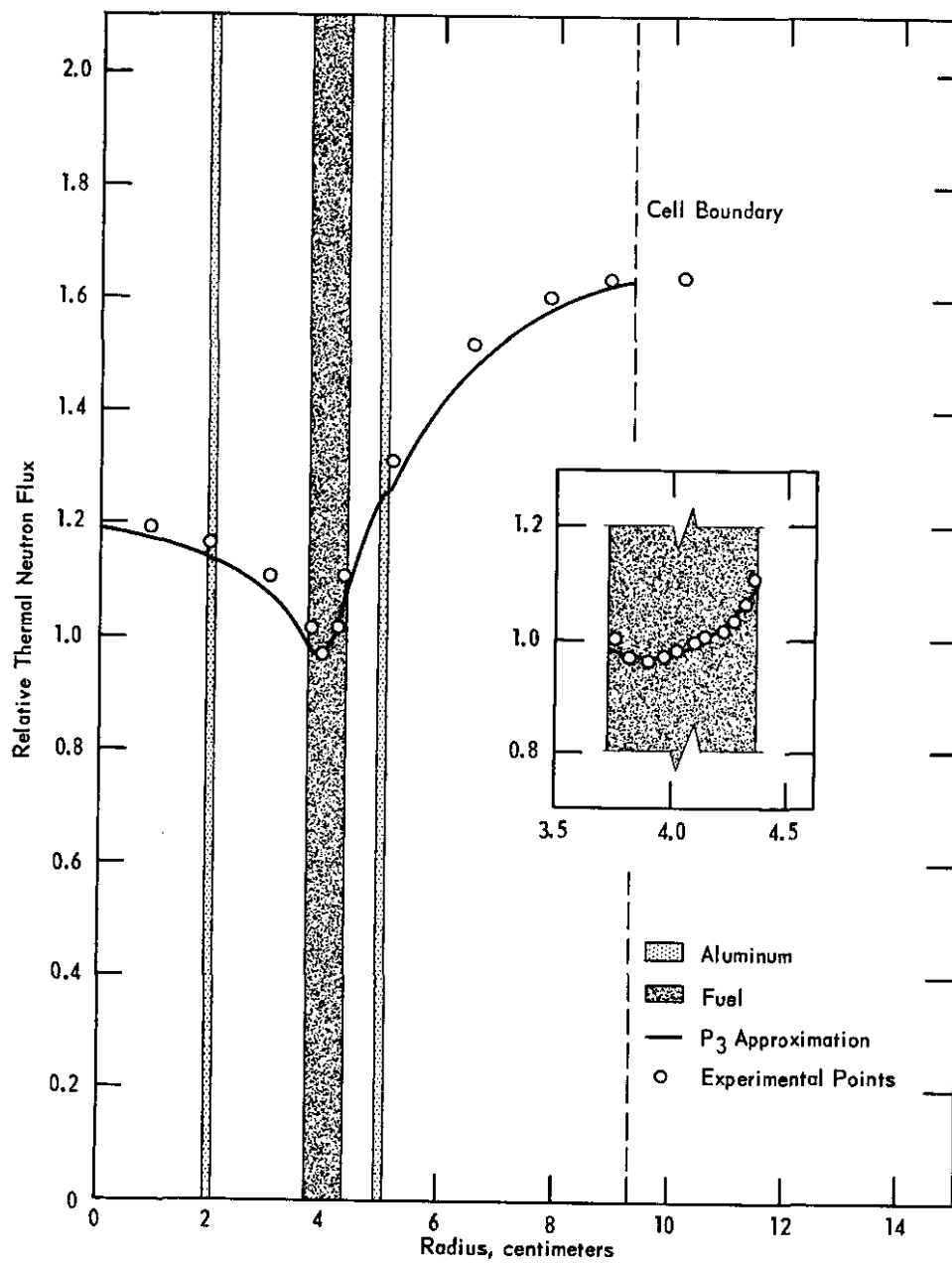


FIG. 6 EXPERIMENTAL AND THEORETICAL FLUX DISTRIBUTIONS - CASE 2

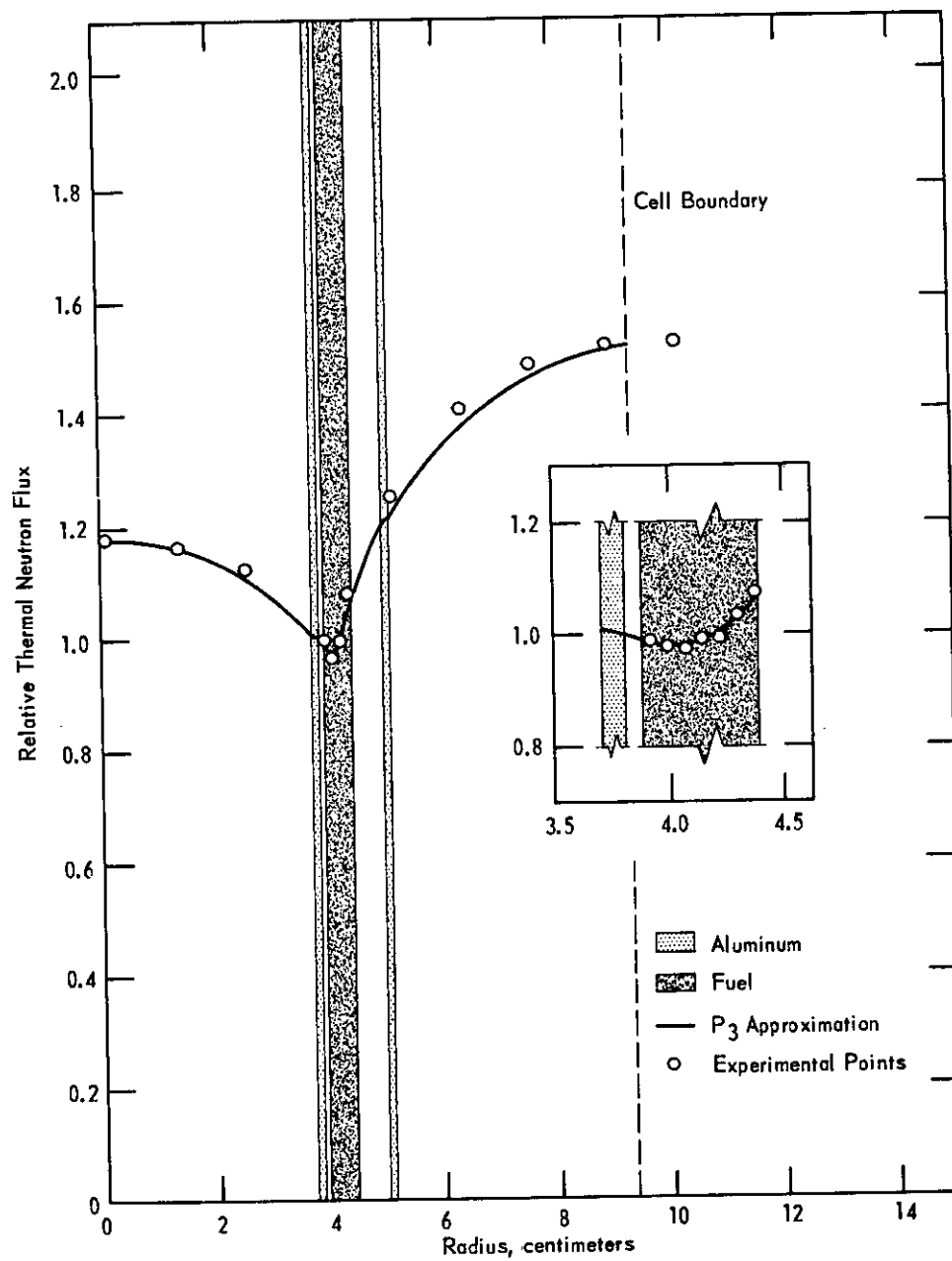


FIG. 7 EXPERIMENTAL AND THEORETICAL FLUX DISTRIBUTIONS - CASE 3

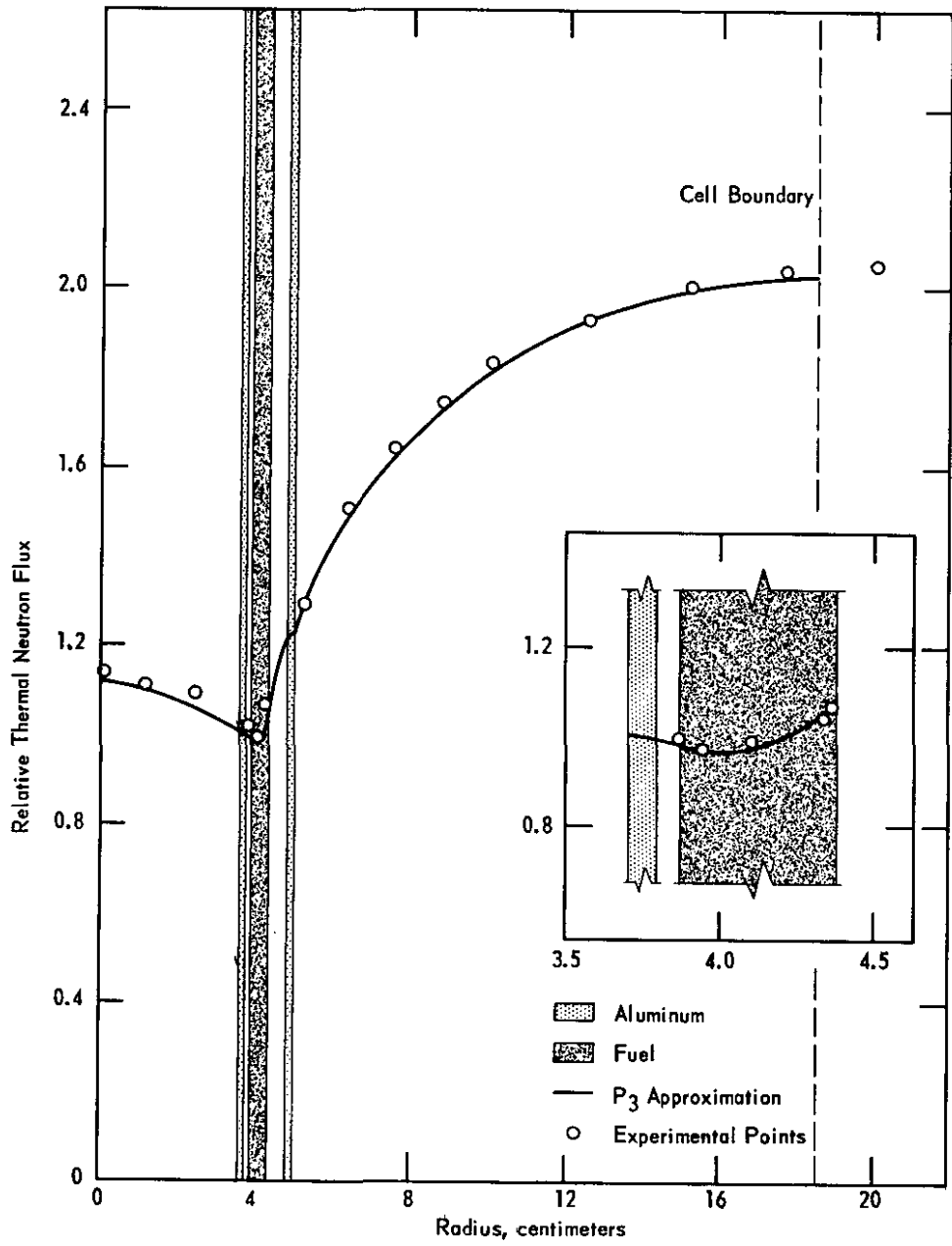


FIG. 8 EXPERIMENTAL AND THEORETICAL FLUX DISTRIBUTIONS - CASE 4

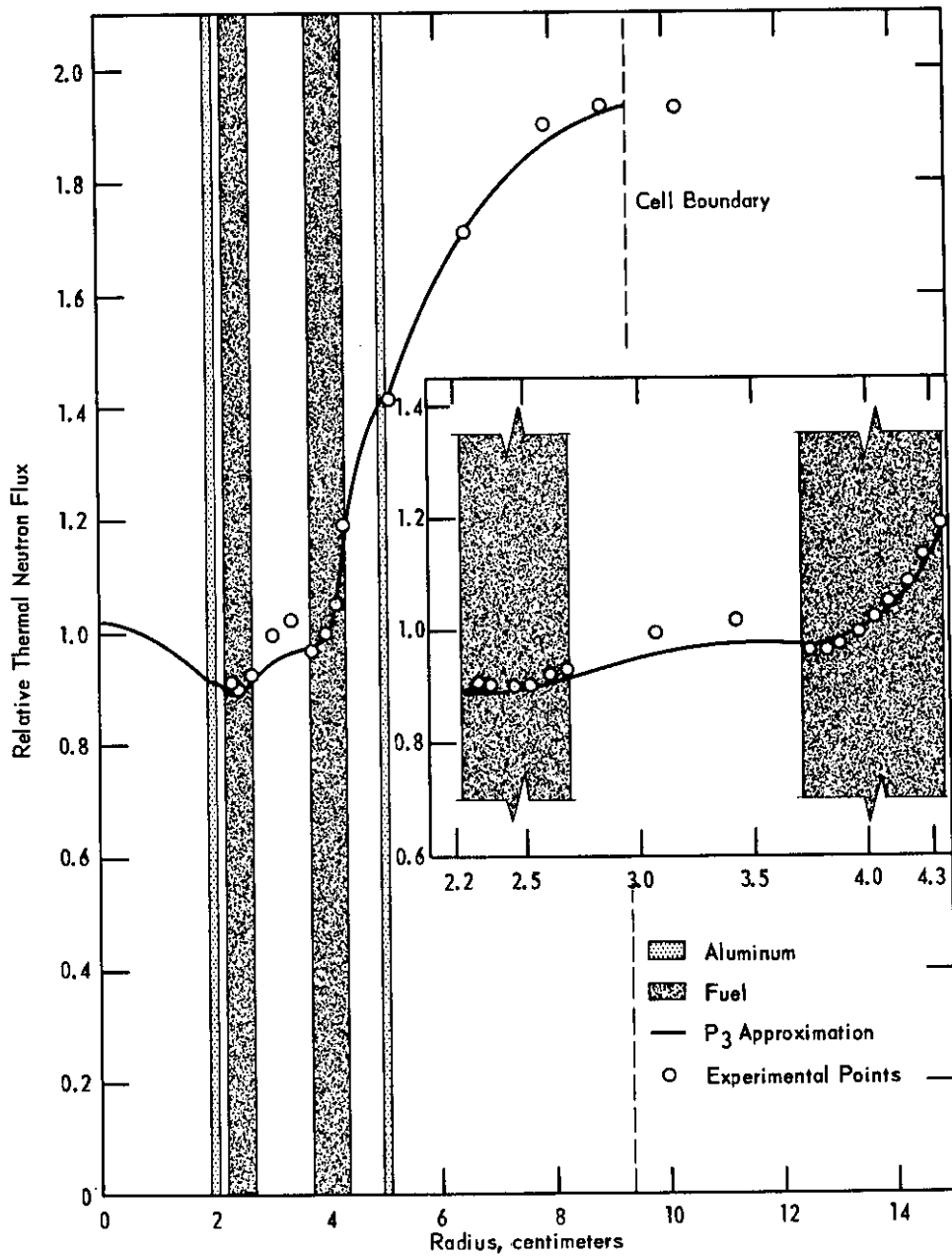


FIG. 9 EXPERIMENTAL AND THEORETICAL FLUX DISTRIBUTIONS - CASE 5

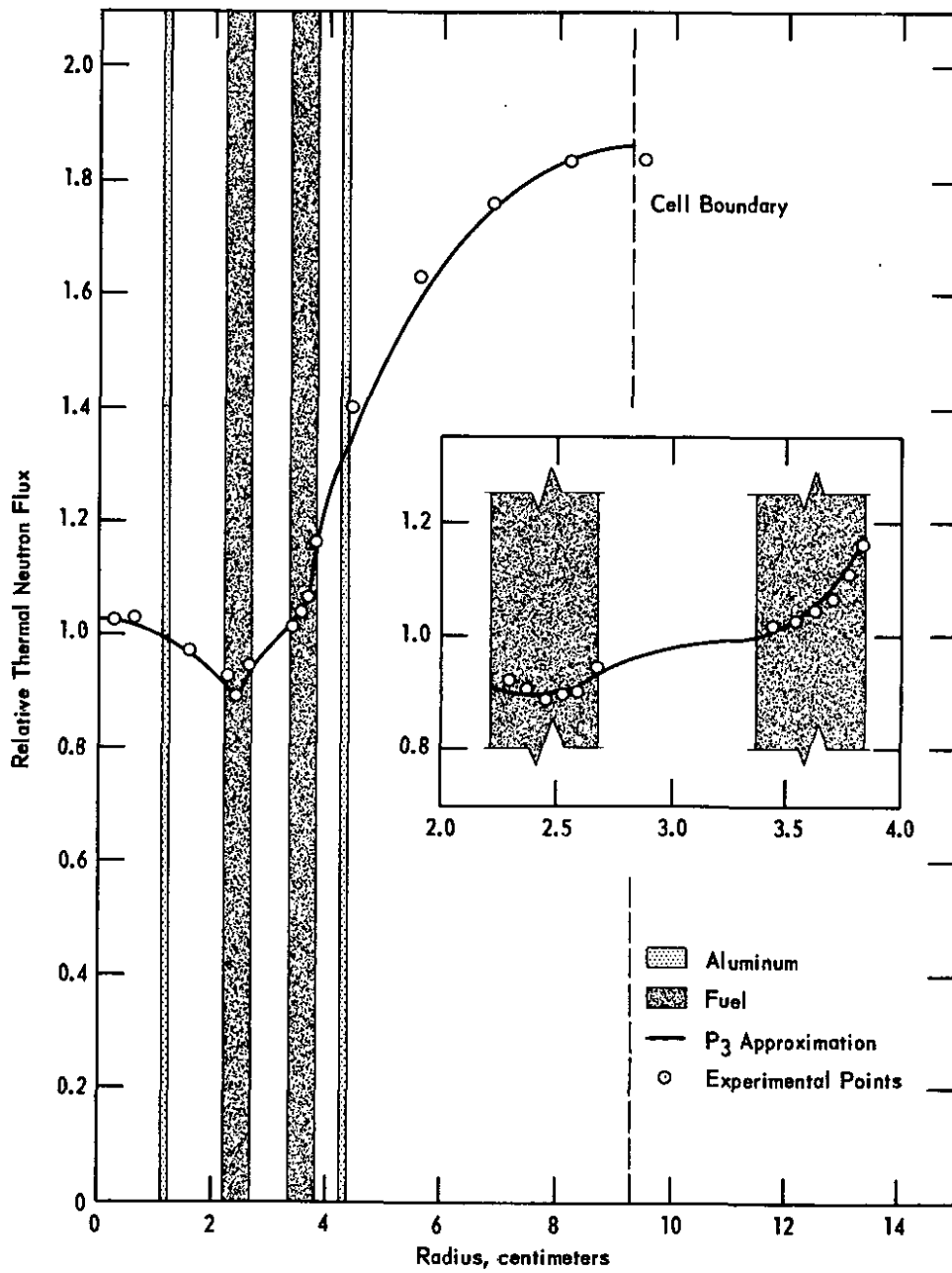


FIG. 10 EXPERIMENTAL AND THEORETICAL FLUX DISTRIBUTIONS - CASE 6

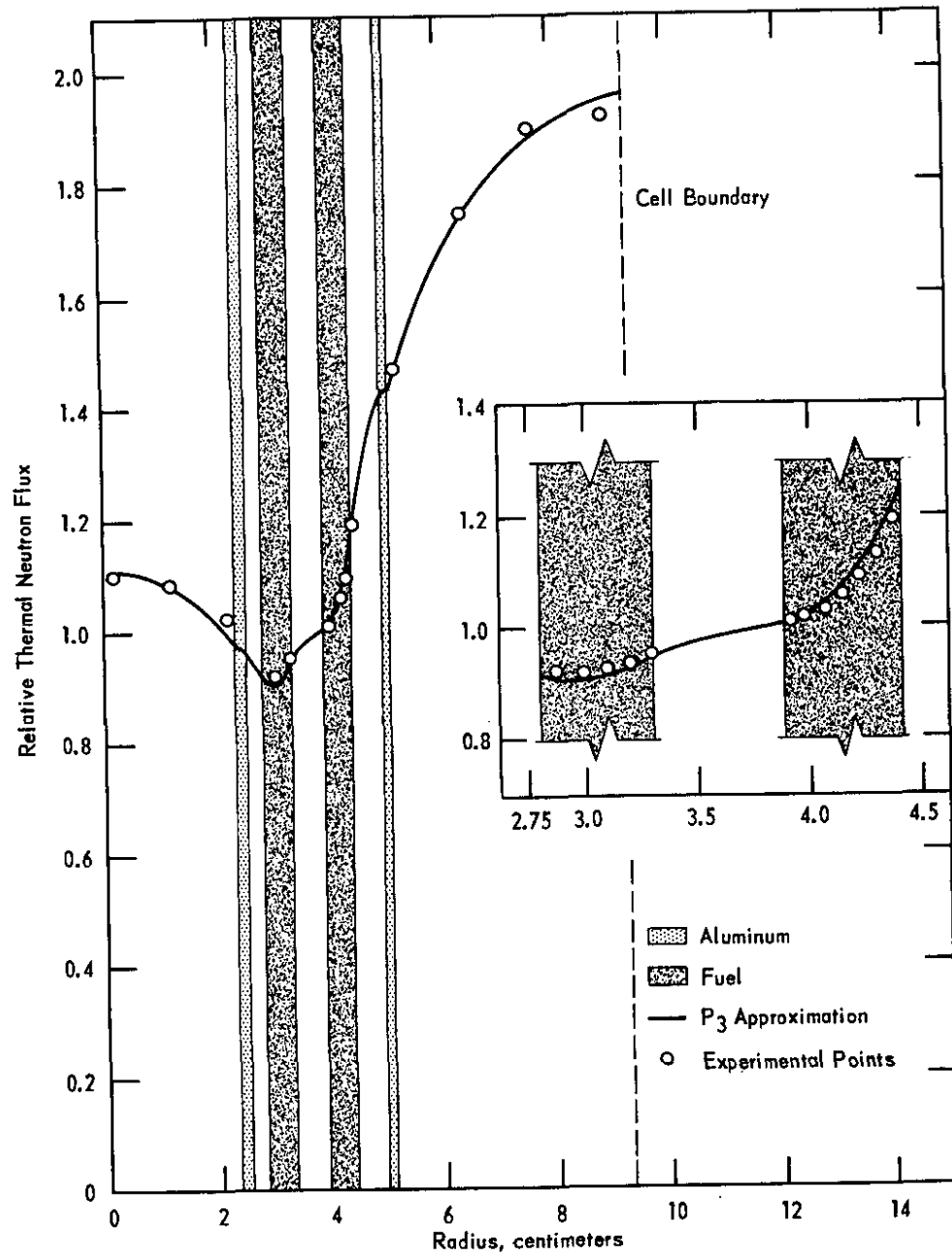


FIG. 11 EXPERIMENTAL AND THEORETICAL FLUX DISTRIBUTIONS - CASE 7

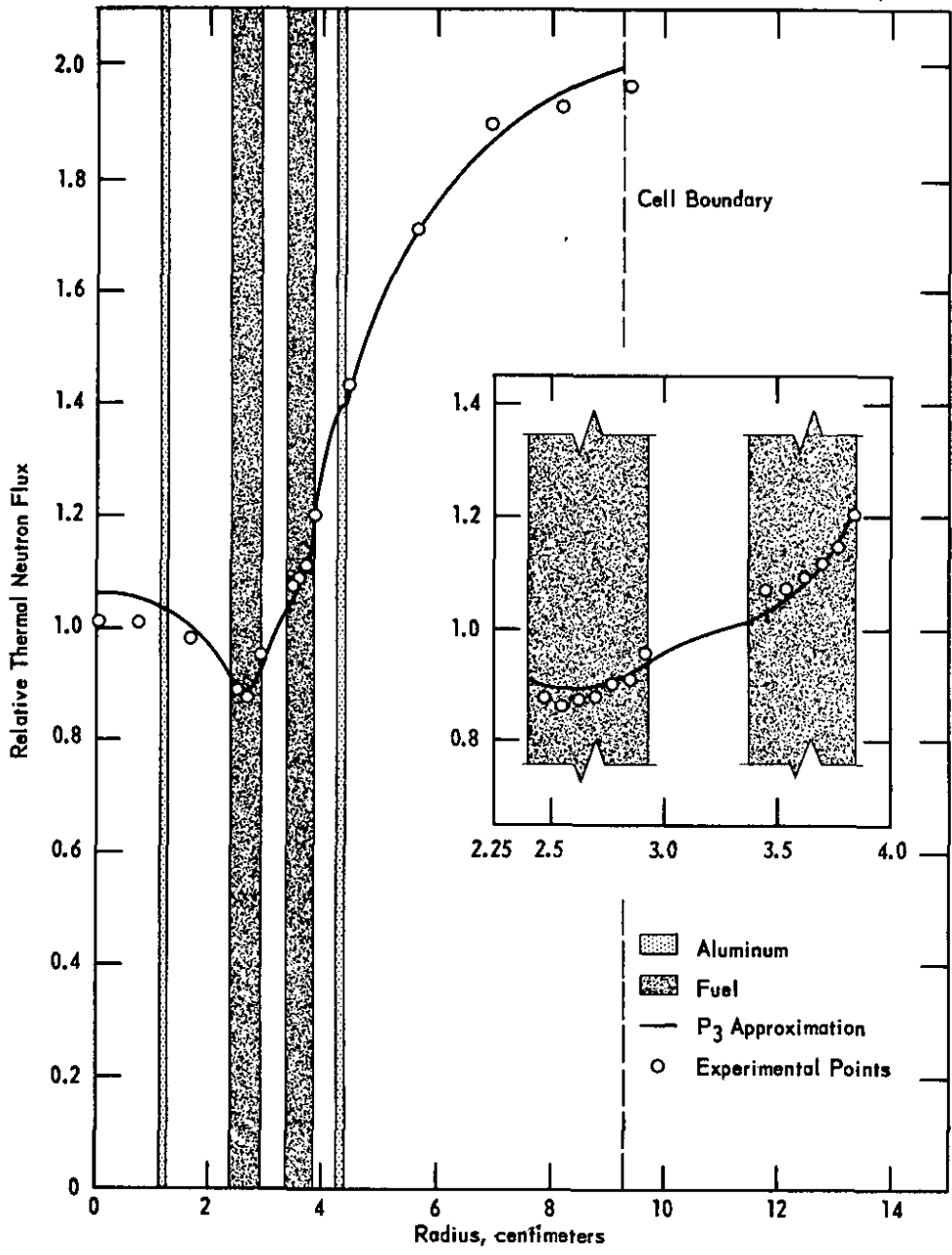


FIG. 12 EXPERIMENTAL AND THEORETICAL FLUX DISTRIBUTIONS - CASE 8

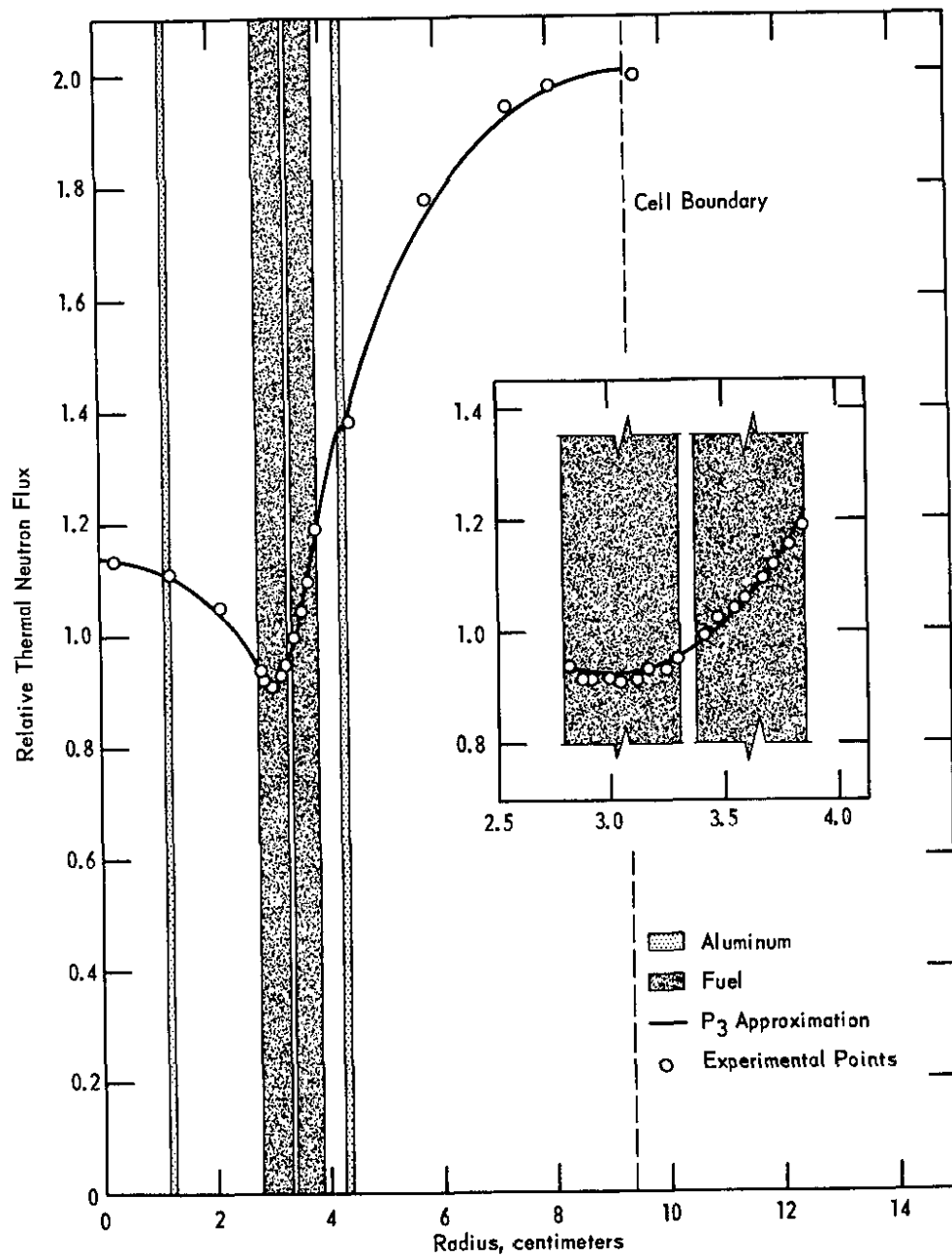


FIG. 13 EXPERIMENTAL AND THEORETICAL FLUX DISTRIBUTIONS - CASE 9

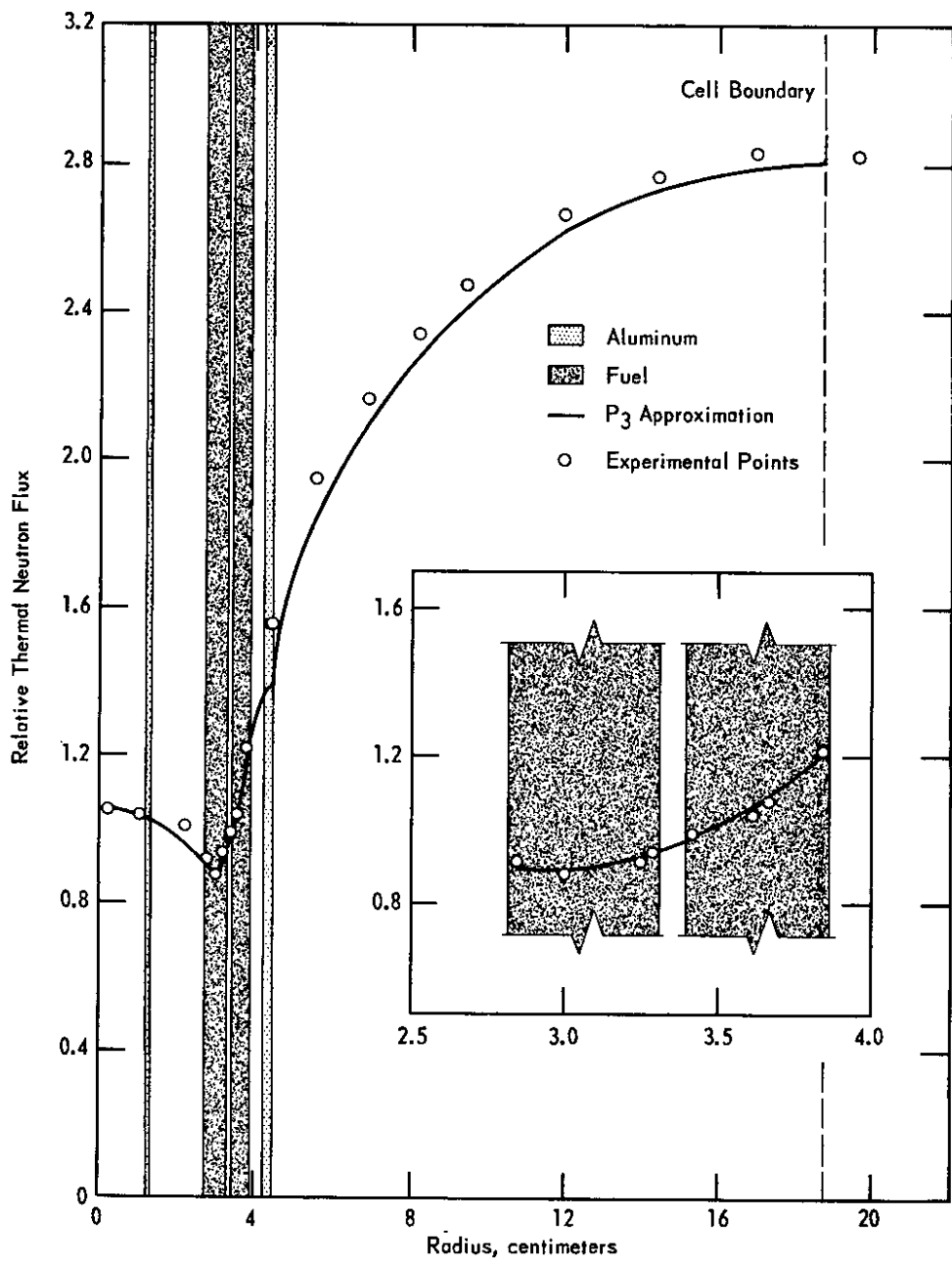


FIG. 14 EXPERIMENTAL AND THEORETICAL FLUX DISTRIBUTIONS - CASE 10

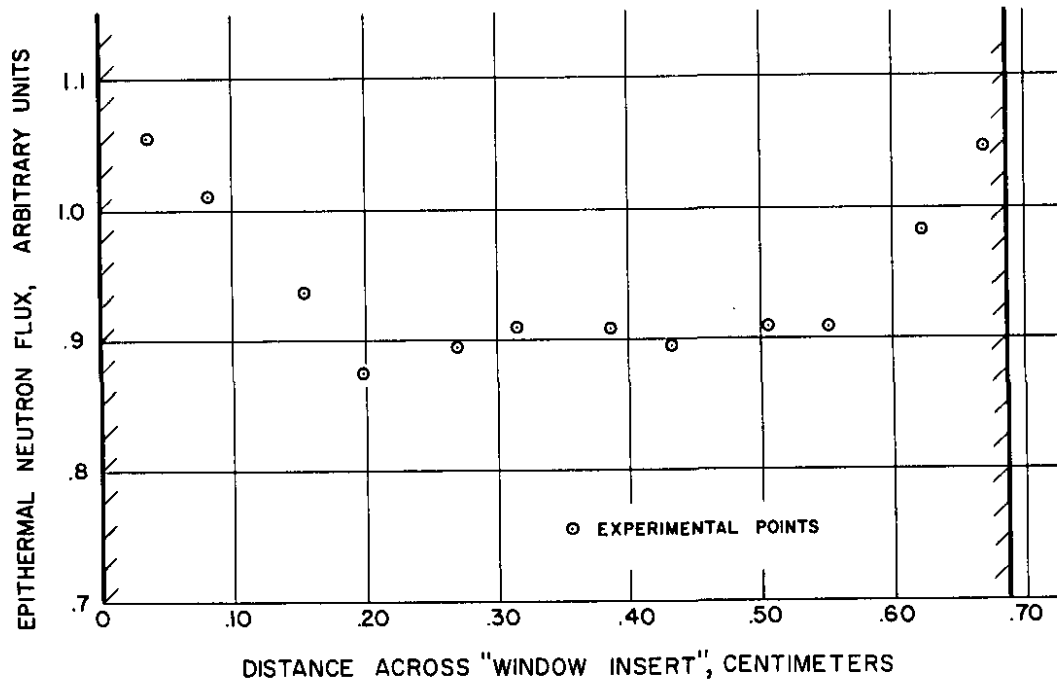


FIG. 15 APPARENT EPITHERMAL FLUX DISTRIBUTION IN THE FUEL REGION TRAVERSED WITH MANGANESE DETECTORS